PHYSICAL REVIEW B **88**, 220412(R) (2013)

Spin-Cherenkov effect and magnonic Mach cones

Ming Yan,[1,*] Attila Kákay,[2] Christian Andreas,[2,3] and Riccardo Hertel[3]
[1]*Department of Physics, Shanghai University, Shanghai 200444, China*
[2]*Peter Grünberg Institut (PGI-6), Forschungszentrum Jülich GmbH, D-52428 Jülich, Germany*
[3]*Institut de Physique et Chimie des Matériaux de Strasbourg, Université de Strasbourg, CNRS UMR 7504, Strasbourg, France*
(Received 5 November 2012; revised manuscript received 27 September 2013; published 30 December 2013)

We report on the Cherenkov-type excitation of spin waves (SWs) in ferromagnets. Our micromagnetic simulations show that a localized magnetic field pulse moving sufficiently fast along the surface of a ferromagnet generates a SW boom, with a Mach-type cone of propagating wave fronts. The SWs are formed when the velocity of the source exceeds the propagation speed of SWs. Unlike the single cone of the usual Cherenkov effect, we find that the magnetic Mach cone consists of two wave fronts with different wave numbers. In patterned thin strips, this magnetic analog of the Cherenkov effect should enable the excitation of SWs with well-defined and velocity-dependent frequency. It thereby provides a promising route towards tunable SW generation, with important potential for applications in magnonic devices.

DOI: 10.1103/PhysRevB.88.220412 PACS number(s): 75.78.Cd, 75.30.Ds, 41.60.Bq, 43.28.Mw

The Cherenkov effect,[1,2] together with the Doppler effect, belongs to a branch of fundamental physics describing the radiation of uniformly moving sources. As pointed out by Ginzburg,[3] these phenomena are universal in physics. Awarded with the Nobel Prize in 1958, the Cherenkov effect now plays a significant role in many disciplines. It is mainly exploited in particle physics, where detectors based on Cherenkov radiation are indispensable to identify high-energy particles. The effect is considered to be rooted so fundamentally in physics, that it has been at the center of an argument brought up against the suspected observation of superluminal neutrinos[4] that was reported recently and broadly discussed in the media.[5]

The characteristic property of the Cherenkov effect is the spontaneous emission of radiation, with wave fronts propagating along a symmetric cone with a moving pointlike source at the apex. The spontaneous emission of electromagnetic waves occurs when a charged particle moves through a dielectric medium at a speed above the phase velocity of light. Hence, the phenomenon is deeply rooted in high-energy physics and is inherently of relativistic nature. It can nevertheless occur in an almost identical fashion also in classical systems, as in the case when an aircraft, a rocket, or a bullet trespasses the speed of sound. This is also comparable to the Doppler effect, which occurs in classical physics as well as in a relativistic version, with the latter being of utmost importance in astronomy. In a more general definition, the Cherenkov effect can be considered as spontaneous radiation which unfolds when a source travels through a medium faster than the propagation speed of the fundamental wave excitation of this medium. As a variant of this effect in condensed matter physics, simulations have very recently demonstrated the possibility of Cherenkov radiation of surface polaritons.[6]

In ferromagnetism, while the spin Doppler effect[7] has recently attracted much attention, an analogy to the Cherenkov effect has so far not been investigated. The single report in the literature on this effect is a recent simulation study of an essentially one-dimensional (1D) system: We predicted there that a Cherenkov-type emission of magnons could be generated by a certain type of domain walls forming in magnetic nanotubes[8] of deep submicron diameter. Owing to their exceptional stability, this exotic type of domain wall can propagate faster than magnons, thereby giving rise to this interaction. This particular type of domain wall is the only micromagnetic structure known to date with such properties. Therefore this first indication of the Cherenkov effect in magnetic systems was limited to the motion of a special type of domain wall, developing only in an even more special geometry. Here we significantly broaden the subject by showing that the Cherenkov emission of spin waves (SWs) in a ferromagnet is a general phenomenon which neither requires a moving domain wall nor a special tubular geometry to unfold.

The continuum theory of micromagnetics describes the magnetic order of the system by the vector field of the magnetization, whose dynamics is driven by an effective field. Any moving source interacting with the spins will result in a perturbation of the magnetic order of the system. The interaction of a moving source on a magnetic sample can hence effectively be represented by a localized magnetic field pulse traveling through the medium or along its surface.[9] This model of a localized and moving field pulse provides a suitable approach to study the general features of the Spin-Cherenkov effect (SCE), encompassing a variety of possible sources that could give rise to this effect. The list of stimuli includes electric currents, electron beams,[10,11] domain walls,[12–14] scanning laser beams,[15] or magnetic monopoles.[16,17] In all these cases, the excitation of SWs can be considered as the response of the magnetic system to a moving field pulse. Within this framework, the Cherenkov radiation of SWs can be recognized as a resonance effect. For simplicity, we consider a field pulse that runs with constant velocity v along a thin-film strip, where the latter serves as a 1D waveguide. For any arbitrary pulse shape $h(x)$, we assume Galilei invariance with the pulse moving according to $h(x - vt)$, where t is the time. The coupling between the field pulse and SW modes, which in this case are 1D propagating plane waves, can be represented by the integral

$$\int_{-\infty}^{+\infty} dx \int_{-\infty}^{+\infty} dt\, h(x - vt) e^{i(kx-\omega t)}, \qquad (1)$$

where k and ω are the wave vector and the radian frequency of the plane waves, respectively. This integral is proportional to $\delta(v - \omega/k)$, where δ denotes the Dirac delta function. This

means that a moving field pulse, or equivalently a moving source with velocity v, can only excite plane waves with a phase velocity $v_p \equiv \omega/k$ equal to v. This wave excitation hence results from the fulfillment of a resonance condition, provided by a *velocity match* in the conventional sense.

To demonstrate the resonance effect discussed above, we performed full three-dimensional (3D) micromagnetic simulations to examine the response of a longitudinally magnetized thin-film strip to a moving field pulse. This corresponds to a pointlike magnetic source moving along the surface, generating a localized field perpendicular to the strip.[18,19] For simplicity, we assume no variation of the field along the film thickness. The magnetization dynamics of the strip is calculated by solving numerically the Landau-Lifshitz-Gilbert equation with our TetraMag finite-element package:[20]

$$\frac{d\vec{M}}{dt} = -\gamma \vec{M} \times \vec{H}_{\text{eff}} + \frac{\alpha}{M_s}\left[\vec{M} \times \frac{d\vec{M}}{dt}\right], \qquad (2)$$

where $\vec{M}$ is the local magnetization, M_s the saturation magnetization, γ the gyromagnetic ratio, $\vec{H}_{\text{eff}}$ the effective field, and α the Gilbert damping factor. Typical material parameters of permalloy, $\mu_0 M_s = 1$ T, exchange constant $A = 1.3 \times 10^{-11}$ J/m, and zero anisotropy are used. The volume is discretized into irregular tetrahedrons of about 3 nm size. The Gilbert damping coefficient α is set to 0.02. As illustrated in Fig. 1, a strong dependence of magnetization dynamics on the pulse velocity v_h is observed. In the low velocity case [$v_h = 500$ m/s in Fig. 1(a)], the pulse only causes a distortion of the magnetization, traveling together with the pulse. No SW is excited. In stark contrast, significant SW excitations are obtained in the high velocity cases $v_h = 1030$ m/s and $v_h = 1180$ m/s, as shown in Figs. 1(b) and 1(c). The excited SWs clearly contain two branches. One branch is in front of the pulse and the other behind, forming a wave packet with an unusual profile. Note that these two SW branches have well-defined, yet different wavelength, as becomes apparent in Fig. 1(c). Shortly after the field pulse is applied, the system reaches a dynamic equilibrium. The wave packet then propagates together with the field pulse smoothly and stably, showing no dispersive effect thereafter. The process of formation and propagation of the wave packet can be observed in an animation in the Supplemental Material.[21] By comparing Figs. 1(b) and 1(c), one also notices that the wavelength of the excited SWs is directly related to v_h. We point out that this result confirms the recently reported SW excitation generated by rapidly moving domain walls in magnetic nanotubes,[8] even though now the geometry is different and the underlying magnetic structure of the strip is homogeneous. Because the moving field pulse used in this study may represent the effect of virtually any type of moving source interacting with the magnetic medium, we deduce that this Cherenkov-type radiation of SWs is a general phenomenon, irrespective of the type of source. In Ref. 8, the bichromatic excitation of SWs was attributed to the SW dispersion in nanotubes. Here we clarify that this characteristic spectrum originates from general features of the SW dispersion relation in magnetic media, with little or no restriction to particular geometries.

In extended and homogeneously magnetized thin films, the SW dispersion relation depends on the angle between the

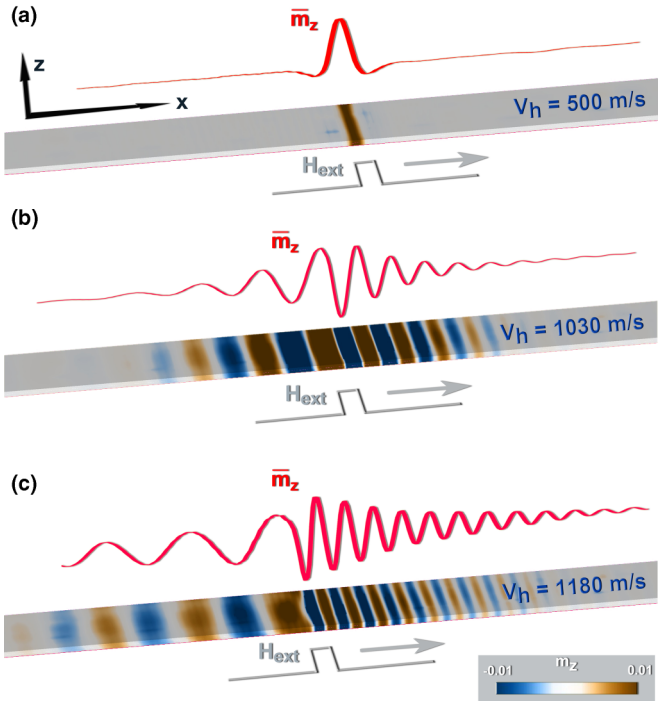

FIG. 1. (Color) Response of the magnetization in a permalloy thin-film strip to a field pulse traveling with constant speed of (a) 500 m/s, (b) 1030 m/s, and (c) 1180 m/s, respectively. The 4-μm-long, 100-nm-wide, and 10-nm-thick strip is magnetized longitudinally, and the field pulse is of rectangular shape, with a magnitude of 10 mT in z direction and 10 nm width in x direction. The color scale represents the z component of the magnetization m_z and the red curves display m_z averaged over the cross section of the strip. The gray line shows the position of the field pulse for each snapshot. The field pulse propagates as indicated by the gray arrows.

propagating direction of the SWs (the wave vector $\vec{k}$) and the magnetization vector $\vec{M}$. The SW modes with $\vec{k}$ perpendicular to $\vec{M}$ are known as Damon-Eshbach modes,[22,23] while those with $\vec{k}$ parallel to $\vec{M}$ are backward-volume modes.[22,24] Despite various differences, the SW modes share some common features. One of them is the nonzero cutoff frequency of the ferromagnetic resonance (FMR) mode, which corresponds to the SW mode at $\vec{k} = 0$. The inset of Fig. 2 displays the numerically calculated SW dispersion relation of the permalloy strip with $\vec{k}$ and $\vec{M}$ parallel to the long axis. The nonvanishing FMR frequency, which is due to the anisotropy of the magnetic system, corresponds to an infinite phase velocity v_p of SWs at $\vec{k} = 0$. The SW dispersion is mainly determined by the interplay of the long-range magnetostatic interaction and the short-range exchange interaction. At large $\vec{k}$, the exchange interaction dominates, yielding a dispersion relation proportional to k^2.[25] This means that in the large $\vec{k}$ region, v_p also tends towards infinity. Therefore $v_p(k)$ must assume a minimum v_0 at a specific nonzero wave vector k_0. This can be seen readily in Fig. 2, where $v_p(k)$ is plotted for a long permalloy nanostrip. The values are extracted from the numerically determined dispersion relation $\omega(k)$. No SW can propagate in the system at velocities below v_0. Therefore, a moving source has to overcome this critical velocity v_0 in order

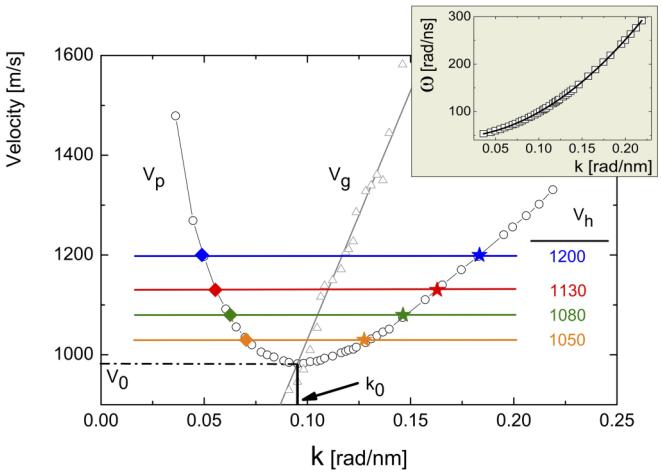

FIG. 2. (Color) Numerically determined phase velocity $v_p(k)$ and group velocity $v_g(k)$ of SWs in a permalloy thin-film strip, which is 4 μm long, 100 nm wide, and 10 nm thick. The values of $v_p(k)$ and $v_g(k)$ are extracted from the SW dispersion relation $\omega(k)$ shown in the inset. The lines are guides to the eye. At k_0, where v_p has a minimum v_0, the $v_g(k)$ curve crosses the $v_p(k)$ line. The colored symbols show the wave vectors of the SW tails excited by the moving field pulse applied to the strip at the corresponding speed. The colored horizontal lines, indicating the speed of the field pulse, connect the two SW branches (star in front and diamond behind).

to attain the Cherenkov excitation of SWs. Note that, there is a twofold degeneracy of spin waves with v_p above v_0, which yields the characteristic bichromatic form of the Cherenkov radiation shown in Figs. 1(b) and 1(c) for $v_h > v_0$.

From Fig. 1, one notices that the two SW branches are well separated with the one of larger $\vec{k}$ always in front. This mode separation results from different group velocities v_g of the two SW modes, a feature that is guaranteed by the shape of the SW phase velocity curve $v_p(k)$. With the condition $dv_p/dk|_{k_0} = 0$, it follows that $v_p(k_0) = d\omega/dk|_{k_0} \equiv v_g(k_0)$. Hence, the SW group velocity is equal to the phase velocity at k_0, which is graphically shown by the crossing of the $v_p(k)$ and $v_g(k)$ for the permalloy strip in Fig. 2. For $k \neq k_0$ it follows that $v_g < v_p$ if $k < k_0$ and $v_g > v_p$ if $k > k_0$. Therefore, any two SW modes that are degenerate in their phase velocity with their respective k values bracketing k_0 must have different group velocities. This results in the spontaneous separation of SW branches in the SCE. At the onset of the radiation, two SW modes with equal v_p are excited, forming two SW packets. Due to dispersion, the SW packet with large $\vec{k}$ ($v_g > v_p$) moves to the front of the source and leaves the one with smaller $\vec{k}$ ($v_g < v_p$) behind. After a few nanoseconds, a dynamic equilibrium between spin excitation and dissipation is reached, after which two stable and separated monochromatic branches are formed. This k-vector splitting resembles the phenomenon reported recently by Rubino *et al.* in photonic crystal fibers.[26] As the pulse velocity v_h changes, the SW branches adjust their wavelength and frequency accordingly to match their phase velocity with v_h, as demonstrated in Figs. 1(b) and 1(c). A systematic study with varying v_h shows that the evolution of the SW branches is precisely determined by the dispersion relation. This is illustrated in Fig. 2, where the colored horizontal lines indicate four different values of v_h and the colored symbols correspond to the k vectors of the SW branches excited by the SCE. The SW dispersion is obtained by applying a localized harmonic oscillating field and extracting the wavelength of the resulting monochromatic SWs. The ability to reconstruct the $v_p(k)$ curve by exciting SWs with moving field pulses demonstrates that the two methods of exciting SWs, either by matching their frequency or their velocity, are equivalent.

The simulations of the thin-film strip presented above elucidate the fundamental mechanism and some basic characteristics of the SCE. We now go further and study the SCE in 2D and 3D systems, which allow for the propagation of SWs in different directions. Following the same spirit, we simulate the response of a ferromagnetic thin-film disk and a ferromagnetic ("bulk"-like) rectangular prism to a moving field pulse, respectively. The pulse is spatially localized so that, at any instant, it only affects a small portion of the magnetic sample. This ensures a good approximation for a pointlike moving source. In the 3D case, the field is localized in a small spot at the surface with only a few nanometers penetration depth. In our simulations, the disk and the rectangular prism are homogeneously magnetized and the field pulse moves along the direction of the magnetization. Similar to the 1D case, SWs are excited only when the pulse reaches a critical speed, indicating the same Cherenkov nature of the excitation. Above the critical velocity, the simulations yield radiation profiles of both 2D and 3D SCEs, which are displayed by snapshots of the magnetization in Figs. 3 and 4, respectively. For better visibility, the propagating SWs in the 3D case are shown on inclined cut planes. A half-cone of SW fronts can be recognized ahead and behind the moving field source in the 3D case. The wave fronts in 2D and 3D SCEs are bent, forming a shape which we refer to as the magnonic Mach cone because of its direct analogy to the Mach cone in the sonic boom. As the pulse speed increases, the bending of the wave front becomes more pronounced [cf. Fig. 3(b)]. This is again similar to the sonic Mach cone, which becomes narrower as the aircraft goes faster. Unlike the sound wave or light, however,

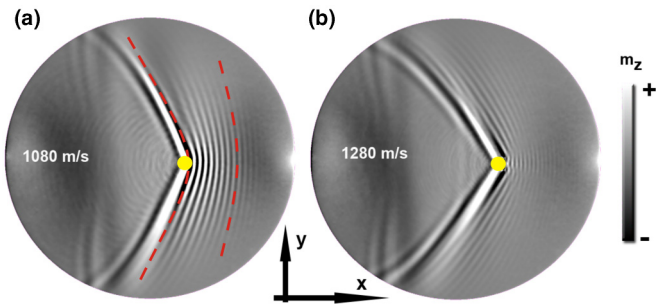

FIG. 3. (Color online) Snapshots of SWs in a permalloy disk (2 μm diameter and 10 nm thickness) induced by a 40 mT field pulse moving with a constant speed of 1080 m/s (a) and 1280 m/s (b). The yellow dots display the position of the field pulse, which is moving in the x direction. As sketched in (a), two bent SW fronts can be identified: one in front of the source and another behind it. In the high velocity case, the wave fronts are distorted and merge, thereby preventing a clear-cut distinction between anticipating and retardating cones.

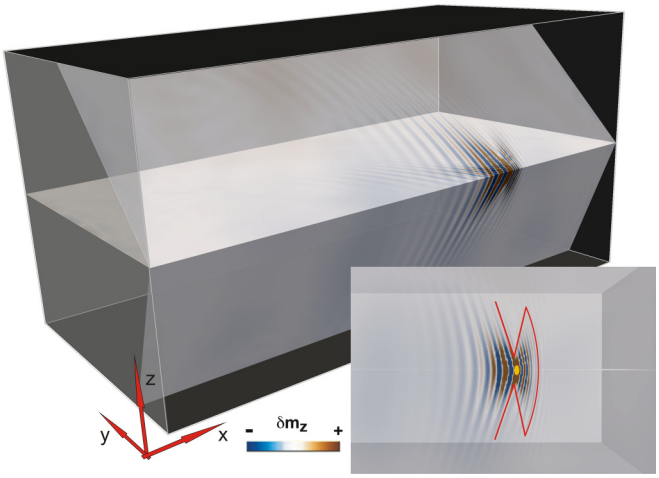

FIG. 4. (Color) Snapshot of the magnetization fluctuations δm_z in a homogeneously magnetized prism (2 μm × 1 μm × 1 μm, cell size: 5 nm). The spin waves are displayed on different cut planes in order to indicate their 3D propagation. The SWs are induced by an 80 mT field pulse moving with a constant speed of 2000 m/s along the surface in x direction. The inset is a close-up of the wave front, where the yellow dot shows the pulse position. As a guide to the eye, the particular form of the SW Mach cone is drawn in red, with one SW front preceding the pulse and another following it.

the SW dispersion is anisotropic, i.e., it depends on the relative direction of wave vector and magnetization. It is therefore more difficult to precisely calculate the wave front in the SCE. But at least qualitatively, the bending of the wave front can be understood rather simply: In 2D and 3D SCEs, the moving source can excite SWs propagating in any direction, as long as the source velocity has a component in that particular direction exceeding the minimum SW phase velocity. Therefore, SWs of wave vectors with larger angle relative to the moving direction of the source can be excited when the source moves faster, resulting in more significant bending of the wave front and a thinner magnonic Mach cone.

Despite the similarity between the magnonic Mach cone and the sonic (or photonic) Mach cone, there is a fundamental difference between them. In the latter ones, the moving source is always located at the apex of the cone, or, in other words, the wave front is always behind the moving source. This is because of the linear dispersion of the sound wave and light, which yields a single-valued phase velocity of the wave. In magnetic media, however, the nonlinear dispersion yields two SW modes for any phase velocity above the magnonic threshold. Once again, the SCE excites SW modes whose *phase* velocity matches the source velocity. Although the SW dispersion is anisotropic, the twofold degeneracy of the SW modes with same phase velocity as well as their unequal *group* velocity are general features, as discussed previously. As shown in Figs. 3 and 4, the waves develop both in front of and behind the source, according to the two branches with different wave numbers. The bichromaticity is therefore a signature of a magnonic Mach cone, which distinguishes it from the sonic boom and the electric-charge-induced Cherenkov effect.

In summary we have derived a general picture of the SCE within the framework of micromagnetic theory. Due to the nonlinear SW dispersion relation, the radiation profile shows a characteristic bichromatic form, a phenomenon which could also apply to wave excitations in other systems with nonlinear wave dispersions. Considering the fundamental interest and potential applications in magnonic devices based on SW propagation, the SCE deserves experimental explorations.[27]

M.Y. acknowledges financial support from NSFC (11374203). A.K. would like to thank Yuriy Mokrousov for the access given to his computer cluster on which the 3D SCE simulations were performed.

*Corresponding author: myan@shu.edu.cn

[1] P. A. Cherenkov, Dokl. Akad. Nauk SSSR **2**, 451 (1934).
[2] P. A. Cherenkov, Phys. Rev. **52**, 378 (1937).
[3] V. L. Ginzburg, Phys.-Usp. **39**, 973 (1996).
[4] A. G. Cohen and S. L. Glashow, Phys. Rev. Lett. **107**, 181803 (2011).
[5] E. S. Reich, Nature **477**, 520 (2011).
[6] S. G. Liu, P. Zhang, W. H. Liu, S. Gong, R. B. Zhong, Y. X. Zhang, and M. Hu, Phys. Rev. Lett. **109**, 153902 (2012).
[7] V. Vlamnick and M. Bailleul, Science **322**, 410 (2008).
[8] M. Yan, C. Andreas, A. Kákay, F. García-Sánchez, and R. Hertel, Appl. Phys. Lett. **99**, 122505 (2011).
[9] The model of a moving field pulse is the simplest and probably most general approach to describe a propagating and localized magnetic perturbation. Other types of excitations, such as moving point dipoles or multipole sources can be considered analogously, but lie outside the scope of the present study.
[10] A. I. Akhiezer, V. G. Bar'yakhtar, and S. V. Peletminskii, Phys. Lett. **4**, 129 (1963).
[11] M. Tsoi, V. S. Tsoi, and P. Wyder, Phys. Rev. B **70**, 012405 (2004).
[12] V. G. Bar'yakhtar and B. A. Ivanov, Pis. Zh. Eksp. Teor. Fiz. **35**, 85 (1982) [JETP Lett. **35**, 101 (1982)].
[13] D. Bouzidi and H. Suhl, Phys. Rev. Lett. **65**, 2587 (1990).
[14] V. G. Bar'yakhtar, M. V. Chetkin, B. A. Ivanov, and S. N. Gadetskii, in *Dynamics of Topological Magnetic Solitons. Experiment and Theory* (Springer, Berlin, 1994), Chap. 4.
[15] I. V. Baryakhtar and A. E. Chubykalo, J. Phys.: Condens. Matter **3**, 1011 (1991).
[16] T. Datta, Phys. Lett. A **103**, 243 (1984).
[17] P. V. Vorob'ev and I. V. Kolokolov, JETP Lett. **67**, 910 (1998).
[18] M. P. Magiera, L. Brendel, D. E. Wolf, and U. Nowak, Europhys. Lett. **95**, 17010 (2011).
[19] C. Fusco, D. E. Wolf, and U. Nowak, Phys. Rev. B **77**, 174426 (2008).
[20] A. Kákay, E. Westphal, and R. Hertel, IEEE Trans. Magn. **46**, 2303 (2010).

[21] See Supplemental Material at http://link.aps.org/supplemental/10.1103/PhysRevB.88.220412 for a movie showing the excitation of SWs by a moving field pulse.

[22] *Spin Dynamics in Confined Magnetic Structures I*, edited by B. Hillebrands and K. Ounadjela (Springer-Verlag, Berlin, 2002).

[23] R. W. Damon and J. R. Eshbach, J. Phys. Chem. Solids **19**, 308 (1961).

[24] B. A. Kalinikos and A. N. Slavin, J. Phys. C **19**, 7013 (1986).

[25] B. Hillebrands and J. Hamrle, in *Handbook of Magnetism and Advanced Magnetic Materials*, edited by H. Kronmüller and S. Parkin (Wiley, New York, 2007).

[26] E. Rubino, J. McLenaghan, S. C. Kehr, F. Belgiorno, D. Townsend, S. Rohr, C. E. Kuklewicz, U. Leonhardt, F. König, and D. Faccio, Phys. Rev. Lett. **108**, 253901 (2012).

[27] For an experimental verification of the SCE, a localized and fast-moving field (generated, e.g., by a magnetic tip) might not be the simplest choice. In principle, any object that interacts with the magnetic medium should trigger the SCE if it moves faster than the minimum SW phase velocity. A possible realization of this could be a laser beam scanning over the surface of magnetic thin films or strips (Ref. 17), which, if it moves sufficiently fast, should yield the SCE and the formation of magnonic Mach cones.